DOI 10.1007/s11182-019-01728-6

Russian Physics Journal, Vol. 62, No. 3, July, 2019 (Russian Original No. 3, March, 2019)

PHYSICS OF MAGNETIC PHENOMENA

MAGNETIC PROPERTIES OF SOFT MAGNETIC ALLOYS 5BDSR AND 82K3HSR

V. A. Svetlichnyi,[1] V. B. Balashov,[1,2] I. N. Lapin,[1] A. É. Sokolov,[3,4] and V. N. Cherepanov[1]

UDC 621.373.826, 621.318.1

The paper explores the size and morphology of microparticles of soft magnetic alloys 5BDSR and 82K3HSR and nanoparticles first obtained from these alloys using pulsed laser ablation in gas. The magnetic properties of particles are studied depending on their size, composition and production method.

Keywords: soft magnetic amorphous and nanocrystalline alloys, 5BDSR, 82K3HSR, microparticles, nanoparticles, pulsed laser ablation, magnetic properties.

INTRODUCTION

Fine magnetic materials have been increasingly used in various technical [1, 2], medical [3, 4] and ecological [5] applications and also in many other fields. For example, in medicine, methods of magnetic drug targeting are being intensively developed as well as magnetic hyperthermia of malignant tumors and different types of diagnostics [6–9]. The interesting applications of magnetic particles in engineering are connected with magnetic fluids with variable rheological properties [10], magnetic fluid lubrications [11]. Also, magnetic materials can be applied in optics owing to changes in their absorption and deflection properties, which stimulates search for new magnetic compositions and methods of their production, both chemical [9, 12, 13] and physical [14–16]. One of new applications of magnetic materials and fluids is the possibility of control for terahertz radiation, visualization [17] and creation of magnetic-field-driven devices, such as polarizers, attenuators, detectors, *etc*. [18].

Highly permeable dispersion materials are rather interesting as active components of magnetic fluids. Among them are, for example, soft magnetic alloys based on 3*d* metals. One of the most known alloys is FINEMET® (Hitachi Metals, Ltd.) nanocrystalline soft magnetic material [19] and FINEMET®-based materials for different electrical engineering applications. Russian analogs are AMAG alloys produced by Asha Metallurgical Plant, Asha, Russia. Among them are nanocrystalline soft magnetic alloy 5BDSR based on Fe and amorphous soft magnetic alloy 82K3HSR based on Co. Magnetic permeability of these alloys is not over 40000 for 5BDSR and 100 000 for 82K3HSR [20].

The aim of this work is to study the morphology and magnetic properties of micro- and nanoparticles of soft magnetic alloys 5BDSR and 82K3HSR. Micron-sized and nanoparticles particles are investigated in this study. The former are obtained by rapid quenching in inert gas and grinding in a ball mill, while the latter – by pulsed laser ablation in argon.

[1]National Research Tomsk State University, Tomsk, Russia, e-mail: v_svetlichnyi@bk.ru; 201kiop@mail.ru; vnch@phys.tsu.ru; [2]Research Institute of Semiconductor Devices, Tomsk, Russia, e-mail: drigalkin53@mail.ru; [3]Kirensky Institute of Physics of the Siberian Branch of the Russian Academy of Sciences, Krasnoyarsk, Russia, e-mail: alexeys@iph.krasn.ru; [4]Siberian Federal University, Krasnoyarsk, Russia. Translated from Izvestiya Vysshikh Uchebnykh Zavedenii, Fizika, No. 3, pp. 26–30, March, 2019. Original article submitted October 15, 2018.

MATERIALS AND METHODS

Initial materials are nanocrystalline (5BDSR based on Fe) and amorphous (82K3HSR based on Co) soft magnetic alloys. These alloys represent cylinders, ribbons obtained by planar flow casting on a cooling roller with the subsequent rapid quenching (in accordance with the appropriate technical conditions) and powders obtained by the melt quenching in inert gas. The X-ray fluorescence analysis performed on a Shimadzu X-ray Fluorescent Spectrometer 1800 (Japan) shows that 5BDSR alloy contains 80% of iron. Alloying with 1–2% boron, 8% silicon and over 10 other alloying elements (Nb, Cu, Co, Mo, Ni) provides its amorphization. 82K3HSR alloy contains 80% of cobalt, boron, silicon and other alloying elements such as Ni, Cr, Fe, C and Ba. The XRD-6000 X-ray Diffractometer from Shimadzu (Japan) is used to investigate the crystalline structure. These investigations show that the samples are mainly in amorphous state, with the low-intensity reflection profiles of metallic iron for nanocrystalline 5BDSR alloy and that of cobalt for amorphous 82K3HSR alloy.

Since micron-sized particles of the initial powders have a wide size distribution, the 5BDSR alloy ribbon was grinded in a ball mill and then fractionized in calibrated sieves. The minimum particle size of 20–40 μm was selected for the experiments.

Nanosized powders were synthesized using a method of pulsed laser ablation (PLA) in gas under atmospheric pressure. The metal target was placed in a quartz cylindrical reactor in which argon was pumped. The gas flow rate through the reactor was 6–10 ml/min. Excitation of the metal target was achieved by Nd:YAG laser (1064 nm, 7 ns, 150 mJ, 20 Hz) focused by a long-focus lens (F = 500 mm). The laser beam was introduced in the end of the reactor through a polyethylene membrane. After an 8-hour synthesis, the powder nanoparticles were collected from the reactor walls. In order to accelerate the deposition of magnetic particles onto the reactor walls, permanent magnets were mounted to the outer walls of the reactor. The synthesis of nanopowders by pulsed laser ablation in gas and the experimental setup were in detail described in [21].

The morphology of micropowders was studied on a VEGA 3 SBH scanning electron microscope (SEM) (TESCAN, Czech Republic), without the additional sample preparation. The morphology, shape, and size of the nanopwder were analyzed by in a HT-7700 (Hitachi, Japan) transmission electron microscope (TEM) with an energy dispersive X-ray spectrometer attached. The nanopowder was exposed to ultrasound, after that it was dispersed in ethanol and then deposited on copper grids coated with amorphous polymer film.

The magnetic measurements of nanopowders were made using a vibration magnetometer. The powders were mixed with a non-magnetic binder and then compacted into cylindrical pellets. The experimental technique of studying the magnetic properties of nanopowders and the description of the experimental setup were described in [22].

RESULTS AND DISCUSSION

SEM images of the surface morphology and the particle size are presented in Fig. 1. One can see that particles produced by the melt rapid quenching in argon are mostly spherical both for 5BDSR and 82K3HSR alloys, whereas the powder synthesized in the ball mill comprises particles of various shape. Fractionation in calibrated sieves restricts the size range rather properly, especially for spherical particles. The powder obtained after grinding in the ball mill contains a portion of coarse particles.

TEM observations of the nanoparticle morphology obtained *via* pulsed laser ablation in argon (Fig. 2), show that it contains a few amount of coarse spherical particles 100 and 200 nm in size, respectively for 5BDSR and 82K3HSR alloy samples (see Fig. 2*a*, *b*). Most particles are extremely fine having the size of 10 nm for 5BDSR and 15–25 nm for 82K3HSR alloy samples (see Fig. 2*c*, *d*).

The analysis of the space distribution of elements, namely Fe, Si, Nb, Cr, Co in 5BDSR and Co, Fe, Si, Cr in 82K3HSR samples shows that this distribution is uniform and corresponds that shown in the images. Therefore, the sample composition remains unchanged. At the same time, a significant amount of oxygen is present in both samples. This is because the nanoparticle oxidation after their extraction from reactor. Interestingly, Co-based 82K3HSR sample oxidizes more strongly although its particles are coarse.

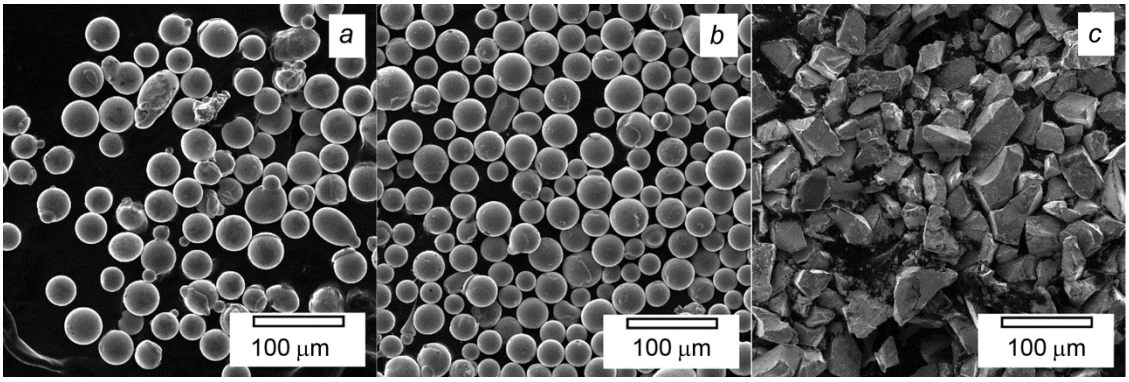

Fig. 1. SEM images of fractionized (20–40 μm) nanoparticles of 5BDSR (*a*) and 82K3HSR (*b*) alloy powders and 5BDSR powder obtained after grinding in the ball mill (*c*).

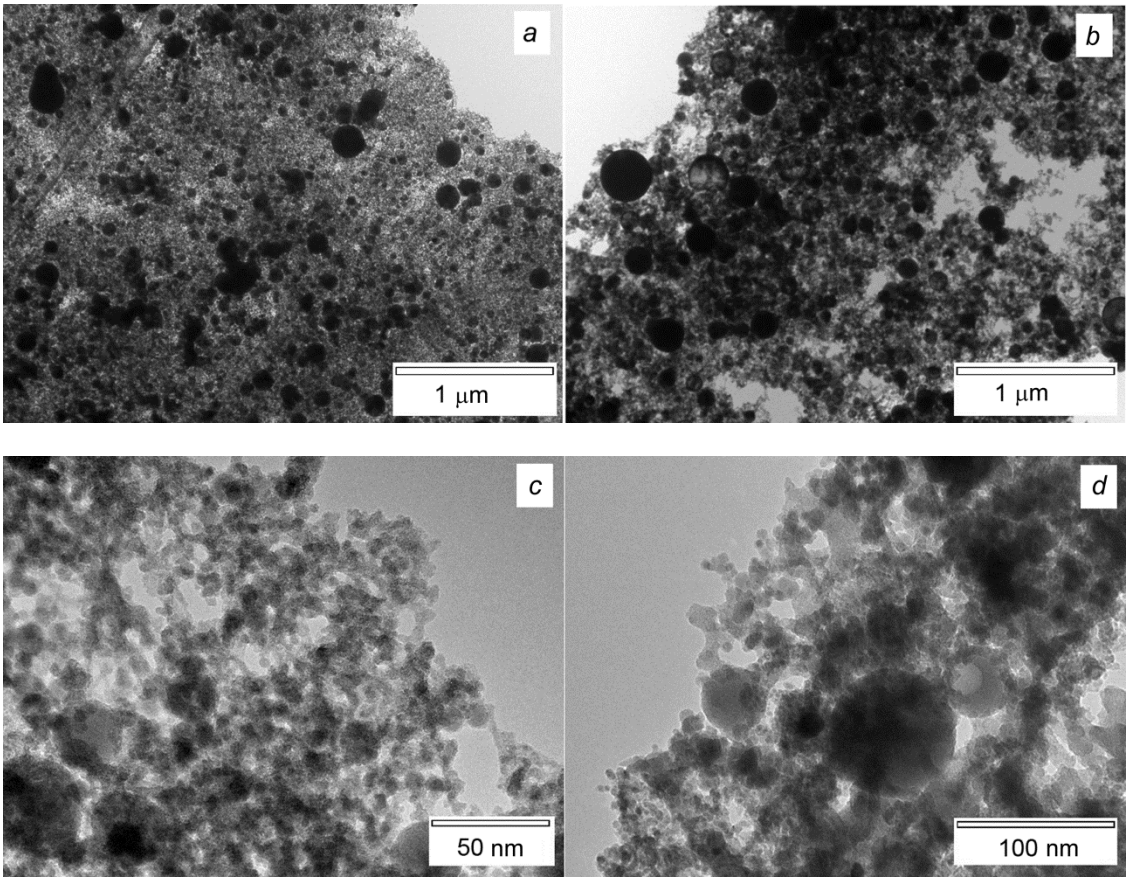

Fig. 2. Overview and refined TEM images of 5BDSR (*a*, *c*) and 82K3HSR (*b*, *d*) alloy particles produced by pulsed laser ablation in argon.

The investigation results of the powder magnetic properties at room temperature are summarized in Table 1 and Fig. 3. Whatever their preparation, 5BDSR micron-sized particles possess the highest saturation magnetization of 140 emu/g. At the same time, these particles obtained by grinding in the ball mill have the lowest coercivity (see Table 1). The residual magnetization of 82K3HSR micron-sized particles is more than 3 times lower than that of

TABLE 1. Magnetic Properties of Soft Magnetic Powders Comprising Micron-Sized and Nanoparticles and Iron Oxide Nanoparticles.

Samples	H_c, Oe	M_s, emu/g	M_r, emu/g
5BDSR micron-sized particles obtained by melt sputtering in Ar	52	140	3.2
82K3HSR micron-sized particles obtained by melt sputtering in Ar	110	30	2.3
5BDSR particles after grinding in a ball mill	18	140	1.4
5BDSR nanoparticles obtained by PLA in Ar	108	10	0.6
82K3HSR nanoparticles obtained by PLA in Ar	100	9	0.6
Fe_3O_4 (magnetite) nanoparticles obtained by PLA in air [15]	100	20	2.8
Fe_3O_4 (magnetite) nanoparticles obtained by PLA in water [15]	145	15	2.5

Note: H_c – coercivity, M_s – saturation magnetization, M_r – residual magnetization.

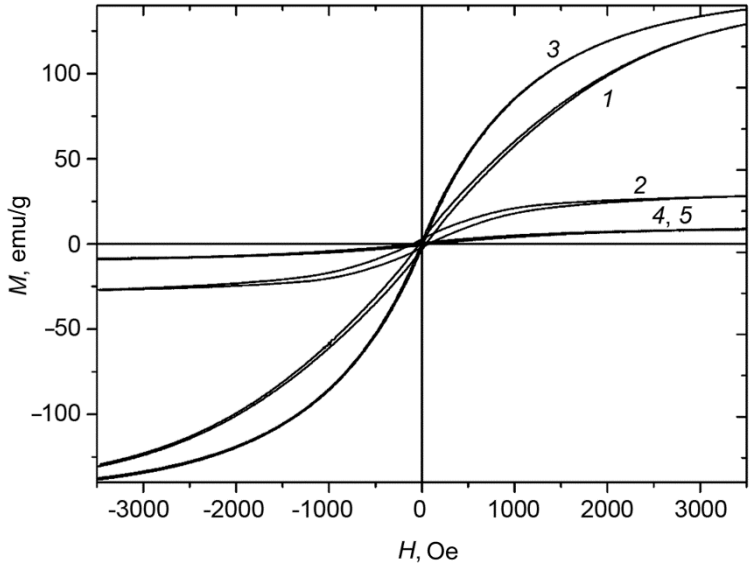

Fig. 3. Dependence between the powder magnetization and magnetic force applied: curves *1* and *2* indicate respectively 5BDSR and 82K3HSR micron-sized particles obtained by melt sputtering in Ar; curve *3* describes 5BDSR micron-sized particles after grinding; curves *4* and *5* indicate 5BDSR and 82K3HSR nanoparticles obtained *via* pulsed laser ablation in Ar.

5BDSR. A narrow hysteresis loop and an insignificant coercivity at room temperature force allow us to refer the investigated micron-sized particles to soft magnetic powders.

During the transition from micro- to nanoparticles, the saturation magnetization of 5BDSR and 82K3HSR powders lowers approximately by 14 times, while the coercivity of 5BDSR powder grows and remains constant for 82K3HSR powder. These changes are associated both with the critical decrease in the particle size and their oxidation.

Table 2 gives the magnetic properties of magnetic Fe_3O_4 nanoparticles produced *via* the pulsed laser ablation of the iron target both in water and in air under almost similar exposure conditions. The saturation magnetization of magnetite nanoparticles is 1.5–2 times higher than that of 5BDSR and 82K3HSR nanoparticles although the latter possess 4–4.6 times lower residual magnetization than Fe_3O_4. Thus, these nanoparticles are considered to be soft magnetic as well as the micron-sized particles.

CONCLUSIONS

Our results described for the first time the synthesis of nanoparticles using the PLA method for soft magnetic alloys 5BDSR and 82K3HSR. The morphology and magnetic properties of 5BDSR and 82K3HSR alloy micron-sized particles were compared to magnetite nanoparticles also obtained by the PLA method. It was shown that nanoparticles obtained by the pulsed laser ablation of 5BDSR and 82K3HSR oxidize after their extraction from the reactor. Being magnetic materials, they possessed the lowest saturation magnetization and coercivity. In order to identify the nature of magnetic properties and possible applications, we intend to continue our research into the composition and structure of the particles and their magnetic properties at different temperatures.

ACKNOWLEDGEMENT

The authors acknowledge the financial support from the Russian Science Foundation (Grant N 18-19-00268) and like to thank their colleagues from Kirensky Institute of Physics SB RAS M. V. Volochaev for his help with TEM measurements and D. A. Velikanov for assistance in measurements on the vibration magnetometer.

REFERENCES

1. J. De Vicente, D. J. Klingenberg, and R. Hidalgo-Alvarez, Soft Matter, **7**, 3701–3710 (2011).
2. B. Ungerbock, S. Fellinger, Philipp Sulzer, *et al.,* Analyst, **139**, No. 10, 2551–2559 (2014).
3. A. Ito, M. Shinkai, H. Honda, and T. Kobayashi, J. Biosci. Bioeng., **100**, No. 1, 1–11 (2005).
4. T. Guo, M. Lin, J. Huang, *et al.,* J. Nanomater., **2018**, 8 (2018). Art. ID 7805147.
5. J. D. Orbell, H. V. Dao, L. N. Ngeh, and S. W. Bigger, Environmentalist, **27**, No. 1, 175–182 (2007).
6. M. Banobre-López, A. Teijeiro, and J. Rivasa, Rep. Pract. Oncol. Radiother., **18**, No. 6, 397–400 (2013).
7. K. Bente, M. Weber, M. Graeser, *et al.,* IEEE Trans. Med. Imaging, **34,** No. 2, 644–651 (2015).
8. T. Takamura, P. J. Ko, J. Sharma, *et al.,* Sensors, **15**, No. 6, 12983–12998 (2015).
9. J. Mosayebi, M. Kiyasatfar, and S. Laurent, Adv. Healthc. Mater., **6**, 80 (2017). Art. ID 1700306.
10. G. Bossis, S. Lacis, A. Meunier, and O. Volkova, JMMM, **252**, 224–228 (2002).
11. X. Shi, W. Huang, and X. Wang, Lubr. Sci., **30**, No. 2, 73–82 (2017).
12. J. Kudr, Y. Haddad, L. Richtera, *et al.,* J. Nanomater., **7**, No. 9, 29 (2017). Art. ID 243.
13. V. A. Zhuravlev, V. I. Itin, R. V. Minin, *et al.,* J. Alloy. Compd., **771**, 686–698 (2019).
14. Y. A. Kotov, J. Nanopart. Res., **5,** No. 5, 539–550 (2003).
15. V. A. Svetlichnyi, A. V. Shabalina, I. N. Lapin, *et al.,* Appl. Surf. Sci., **467–468**, 402–410 (2019).
16. V. A. Svetlichnyi, A. V. Shabalina, and I. N. Lapin, Russ. Phys. J., **59**, No. 12, 2012-2016 (2017).
17. R. Zhang, L. Zhang, T. Wu, *et al.,* Opt. Express, **24**, No. 8, 7915–7921 (2016).
18. M. Shalaby, M. Peccianti, Y. Ozturk, *et al.,* Appl. Phys. Lett., **105**, 3 (2014). Art. ID 151108.
19. M. Rubinstein, V. G. Harris, and P. Lubitz, JMMM, **234**, 306–312 (2001).
20. V. V. Karasev, V. A. Makarov, A. E. Filippov, and V. V. Markin, Elektrotekhnika, No. 4. 51–55 (1994).
21. V. A. Svetlichnyi, A. V. Shabalina, I. N. Lapin, *et al.,* Appl. Surf. Sci., **462**, 226–236 (2018).
22. V. A. Svetlichnyi, A. V. Shabalina, I. N. Lapin, *et al.,* Appl. Phys. A-Mater., **123**, No. 12, 8 (2017). Art. ID 763.